Time Series Modeling and Forecasting of Monthly Mean Sea Level (1978 – 2020): SARIMA and Multilayer Perceptron Neural Network

Yeong Nain Chi [a,1,*]

[a] Department of Agriculture, Food, and Resource Sciences, University of Maryland Eastern Shore, Princess Anne, MD 21853, United States
[1] ychi@umes.edu
* corresponding author

ARTICLE INFO

Article history
Received January 15, 2022
Revised March 7, 2022
Accepted June 10, 2022

Keywords
time series modeling
forecasting
seasonal ARIMA
multilayer perceptron neural network
mean sea level
Grand Isle
Louisiana

ABSTRACT

The primary purpose of this study was to demonstrate the role of time series model in predicting process and to pursue analysis of time series data using long-term records of monthly mean sea level from January 1978 to October 2020 at Grand Isle, Louisiana. Following the Box–Jenkins methodology, the ARIMA (1,1,1)(2,0,0) with drift model was selected to be the best fitting model for the time series, according to the lowest AIC value in this study. Empirically, the results revealed that the MLP neural network model performed better compared to the ARIMA(1,1,1)(2,0,0) with drift model at its smaller MSE value. Hence, the MLP neural network model not only can provided information which are important in decision making process related to the future sea level change impacts, but also can be employed in forecasting the future performance for local mean sea level change outcomes. Understanding past sea level is important for the analysis of current and future sea level changes. In order to sustain these observations, research programs utilizing the resulting data should be able to improve significantly our understanding and narrow projections of future sea level rise and variability.

1. Introduction

Climate change is the long-term change in the average weather patterns of the earth. It is primarily triggered by human activities like burning of fossil fuels, deforestation, etc. or natural events like volcanic eruptions. National Oceanic and Atmospheric Administration (NOAA) 2019 Global Climate Annual Report (https://www.ncdc.noaa.gov/sotc/global/201913) summarized that the global annual temperature has increased at an average rate of 0.07°C (0.13°F) per decade since 1880. This rate (+0.18°C / +0.32°F) of increase has doubled since 1981.

There are two major factors related to climate change caused sea level rise globally: the added water from ice melting from land (ice sheets and glaciers) into the ocean, and the thermal expansion of warming waters. Locally, the amount and speed of sea level rise varies by location, particularly, the slowing Gulf Stream and sinking land affect some areas at varying rates in the United States (https://sealevelrise.org/). The potential impacts of sea level rise include, but not limited to, increasing coastal flooding and erosion, damages on agricultural land cover and crops, damages on coastal/urban settlements and infrastructures, and damages on coastal flora and fauna ecosystems (Neumann et al., 2020).

According to NOAA Climate.gov, global average sea level has risen about 8-9 inches (21-24 cm) since 1880. The Intergovernmental Panel on Climate Change (IPCC) (2014) estimated that the sea level has risen by 26-55 cm (10-22 inches) with a 67% confidence interval. If emissions remain very high, the IPCC projected sea level could rise by 52-98 cm (20-39 inches). In its Fourth National Climate Assessment Report (2017) the U.S. Global Change Research Program (USGCRP) estimated that sea level has risen by about 7-8 inches (about 16-21 cm) since 1900, with about 3 of those inches (about 7 cm) occurring since 1993 (very high confidence). Relative to the year 2000, sea level was very likely to rise by 1.0-4.3 feet (30-130 cm) in 2100, and 0.3-0.6 feet (9-18 cm) by 2030.

There were many studies pointed out that sea level is rising at an increasing rate (Church et al., 2004) (Church & White, 2006) (Church et al., 2008) (Cazenave & Llovel, 2010) (Church & White, 2011) (Cazenave & Cozannet, 2013) (Horton et al., 2018) (Kulp & Strauss, 2019) (Haasnoot et al., 2020). Thus, understanding past sea level is important for the analysis of current and future sea level changes. Modeling sea level changes and understanding its causes has considerably improved in the recent years, essentially because new in situ and remote sensing observations have become available (Foster & Brown, 2014) (Visser et al., 2015) (Bolin et al., 2015) (Srivastava et al., 2016). Despite the importance of sea level rise and its consequences, there is a lack of studies in the technical literature available on forecasting schemes at the local consideration.

Time series analysis comprises methods for analyzing time series in order to extract meaningful statistics of the time series data, while time series forecasting is the use of a model to predict future values based on previously observed values. Furthermore, neural networks have become one of the most popular trends in machine learning for time series modeling and forecasting. Recently, there is increasing interest in using neural networks to model and forecast time series, particularly in the sea level rise issues (Makarynskyy et al., 2004) (Braakmann-Folgmann et al., 2017) (Wang & Yuan, 2018) (Bruneau et al., 2020). Hence, the primary purpose of this study was to demonstrate the role of time series model in predicting process and to pursue analysis of time series data using long-term records of monthly mean sea level from January 1978 to October 2020 at Grand Isle, Louisiana.

2. Materials

2.1 Study Site

Grand Isle is a town in Jefferson Parish, Louisiana, at latitude 29.2366 and longitude -89.9873, located on a barrier island at the mouth of Barataria Bay where it meets the Gulf of Mexico (Figure 1). According to the U. S. Census Bureau, it covered a total area of 7.8 square miles (20 km^2), of which 6.1 square miles (16 km^2) is land and 1.7 square miles (4.4 km^2) is water. Grand Isle has a humid subtropical climate bordering on a tropical monsoon climate, with mild winters and long, hot, humid summers. It has been repeatedly hit by hurricanes through its history. On average, Grand Isle has been affected by tropical storms or hurricanes every 2.68 years since 1877, with direct hit on average every 7.88 years.

2.2 Data Source

The long-term records of monthly mean sea level from January 1978 to October 2020 at Grand Isle, Louisiana (Figure 2), is available to the public from NOAA Tides and Currents (https://tidesandcurrents.noaa.gov/). Average monthly mean sea level was -0.1356 mm/year with the standard deviation of 0.1177 mm/year (Minimum: -0.431 mm/year, Maximum: 0.212 mm/year, and Median: -0.1455 mm/year).

According to NOAA Tides and Currents (https://tidesandcurrents.noaa.gov/), mean sea level refers to a tidal datum, which is locally derived based on observations at a tide station, and is typically computed over a 19-year period, known as the National Tidal Datum Epoch (NTDE). Mean sea level as a tidal datum is computed as a mean of hourly water level heights observed over 19-years. Monthly means generated in the datum calculation process, which is used to generate the relative local sea level trends observed at a tide station.

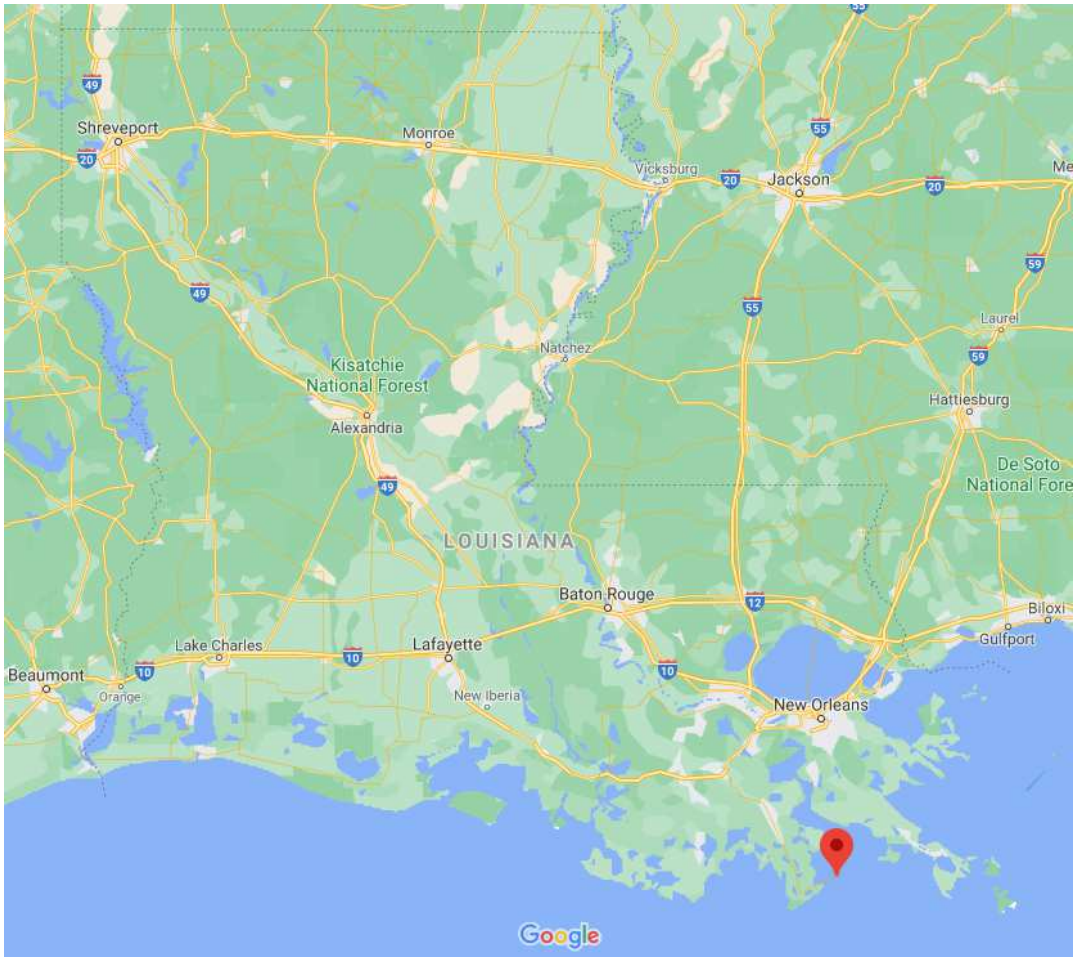

Figure 1. Grand Isle, Louisiana, USA
Source: Google Map (https://www.google.com/maps/place/Grand+Isle,+LA/**)**

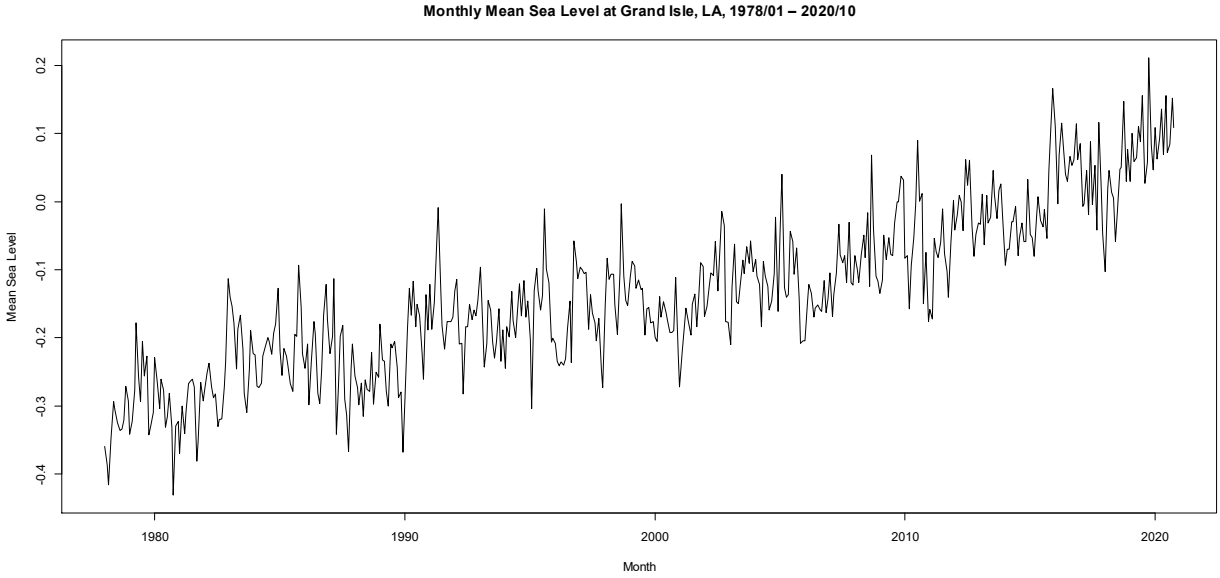

Figure 2. Time Series Plot of Monthly Mean Sea Level at Grand Isle, Louisiana, January 1978 ~ October 2020 (Source: own calculations)

3. Methodology

3.1 Seasonal ARIMA Model

In the Autoregressive Integrated Moving Average (ARIMA) model, the autoregressive process (AR) part indicates that the evolving variable of interest is regressed on its own lagged values; the moving average process (MA) part indicates that the regression error is actually a linear combination of error terms whose values occurred at various times in the past; and the I (for "integrated") part indicates that the data values have been replaced with the difference between their values and the previous values. The purpose of each of these parts is to make the model better fit to predict future points in a time series (Montgomery et al., 2008).

The parameters of the ARIMA (p, d, q) model are defined as: p = the order of the autoregressive process (the number of lagged terms), d = the number of differences required to make the time series stationary, q = the order of the moving average process (the number of lagged terms). In backshift notation B, "backshift operator" or "lag operator", is a useful notational device when working with time series lags: $By_t = y_{t-1}$ (means "back up by one time unit") and $B^k y_t = y_{t-k}$ (means "backshift k times"). Thus, the ARIMA(p,d,q) model can be expressed as:

$$\phi_p(B)(1 - B)^d y_t = c + \theta_q(B)e_t$$

where $\phi_p(B) = (1 - \phi_1 B - \ldots - \phi_p B^p) = (1 - \Sigma^p{}_{i=1}\, \phi_i B^i)$, $\theta_q(B) = (1 - \theta_1 B - \ldots - \theta_q B^q) = (1 - \Sigma^q{}_{j=1}\, \theta_j B^j)$, c is a constant, and e_t is the residual error (i.e., white noise).

Seasonal ARIMA is an extension of ARIMA that explicitly supports univariate time series with a seasonal component. For the seasonal ARIMA model, ARIMA(p,d,q)(P,D,Q)[m], where P = the order of the seasonal autoregressive process, D = the number of seasonal differences applied to the time series, Q = the order of the seasonal moving average process, and m = the seasonality of the model, i.e., the number of time steps for a single seasonal period. The seasonal ARIMA(p,d,q)(P,D,Q)[m] model can be written in backshift notation as:

$$\phi_p(B)\Phi_p(B^m)(1 - B)^d(1 - B^m)^D y_t = c + \theta_q(B)\Theta_Q(B^m)e_t$$

where $\Phi_P(B^m) = (1 - \Phi_1 B^m - \ldots - \Phi_P B^{mP}) = (1 - \Sigma^P{}_{i=1}\, \Phi_i B^{mi})$, $\Theta_Q(B^m) = (1 - \Theta_1 B^m - \ldots - \Theta_Q B^{mQ}) = (1 - \Sigma^Q{}_{j=1}\, \Theta_j B^j)$.

3.2 Box-Jenkins Methodology

In time series analysis, the Box-Jenkins methodology (Box & Jenkins, 1970) (Figure 3) refers to a systematic method of identifying, fitting, checking, and forecasting ARIMA models (Box et al., 2016), that can be applied to find the best fit of a time series. The Box-Jenkins methodology can be used as the process for estimating the seasonal ARIMA model in this study based on its autocorrelation function (ACF) and partial autocorrelation function (PACF) as a means of determining the stationarity of the univariate time series and the lag lengths of the seasonal ARIMA model.

In data analysis, a common assumption is that the time series is stationary. Intuitively, *stationarity* means that the statistical properties (i.e., mean and variance) of the process do not change over time. In statistics, **s**tationarity is a property of a stochastic process. Thus, the Box-Jenkins methodology starts with the assumption that the time series should be as on stationary status. In the Box-Jenkins methodology, there are four important steps, including identification, estimation, diagnostic checking and forecasting, should be put in consideration to apply it.

The identification step applied to achieve stationarity and to build a suitable model using ACFs, PACFs, and transformations (differencing). If the time series is not stationary, it needs to be

stationarized through differencing. In the estimation step, plots and summary statistics can be used to identify trends and autoregressive elements to get an idea of the amount of differencing and the size of the lag that will be required for model identification. The following estimation step is to use a fitting procedure to find the coefficients of the model. In order to discover good parameters for the model, Akaike's Information Criterion (AIC) or Bayesian Information Criterion (BIC) can be employed to determine the orders of a seasonal ARIMA model. Good models are obtained by minimizing the AIC or BIC value.

The diagnostic checking step is primarily to use plots and statistical tests of the residual errors to determine the model fitting, and to evaluate the fitting model in the context of the available data and check for areas where the model may be improved. The process is repeated until a desirable level of fit is achieved. There are many accuracy metrics applied after model identification and estimation helping in choosing the best fitting model. The commonly used accuracy metrics to judge forecasts include: Mean Square Error (MSE) = $(1/n)\ \Sigma(Y_t - \hat{\mathbf{Y}}_t)^2$, Root Mean Square Error (RMSE) = $\sqrt{}$MSE, Mean Absolute Percentage Error (MAPE) = $(1/n)\ \Sigma(|Y_t - \hat{\mathbf{Y}}_t| / |Y_t|)$ *100, and Mean Absolute Error (MAE) = $(1/n)\ \Sigma|Y_t - \hat{\mathbf{Y}}_t|^2$.

The last step is the forecasting step that can be applied in forecasting process after checking the model in the previous steps. In this study, R 4.0.2 for Windows, an open source for statistical computing and graphics supported by the R Foundation for Statistical Computing, was used as the tool to estimate the model parameters to fit the seasonal ARIMA model and the multilayer perceptron neural network model as well to achieve the purpose of this study.

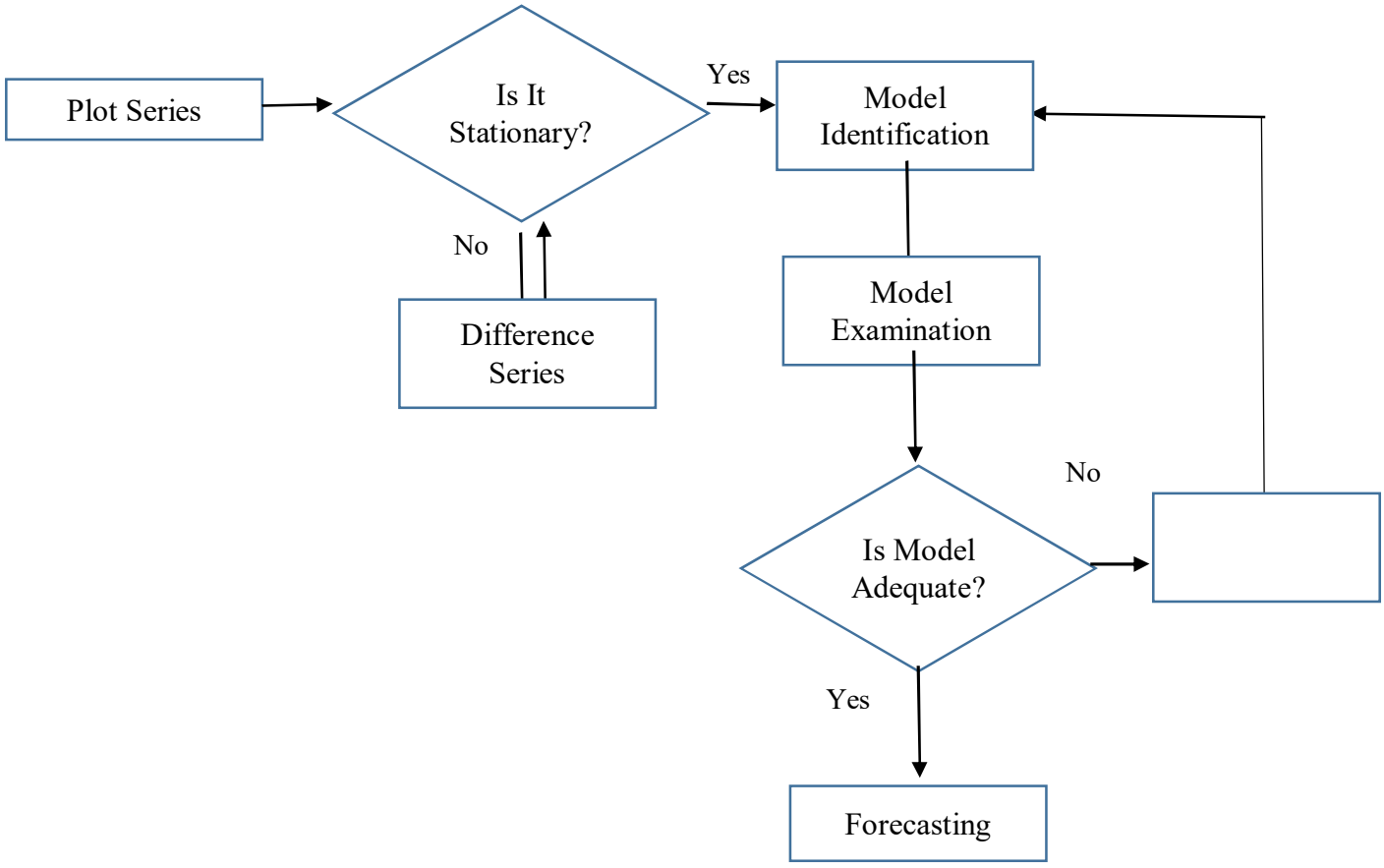

Figure 3. Box-Jenkins Methodology (Source: own calculations)

4. Empirical Results

4.1 Identification of the Seasonal ARIMA Model

R 4.0.2 for Windows is an open source for statistical computing and graphics supported by the R Foundation for Statistical Computing was used as the tool to model and forecast monthly mean sea level from January 1978 to October 2020 at Grand Isle, Louisiana for this study.

A seasonal time series consists of a trend component, a seasonal component and an irregular component. Decomposing the time series means separating the time series into these three components. The function "decompose()" in R can be applied to estimate the seasonal component, trend component and irregular component of a seasonal time series. The plots in Figure 4 showed the original time series (top), the estimated trend component (second from top), the estimated seasonal component (third from top), and the estimated irregular component (bottom). The estimated trend component showed a steady increase over time, and the estimated seasonal component definitely displayed seasonality, with a pattern recurrence occurring once every 12 months (yearly).

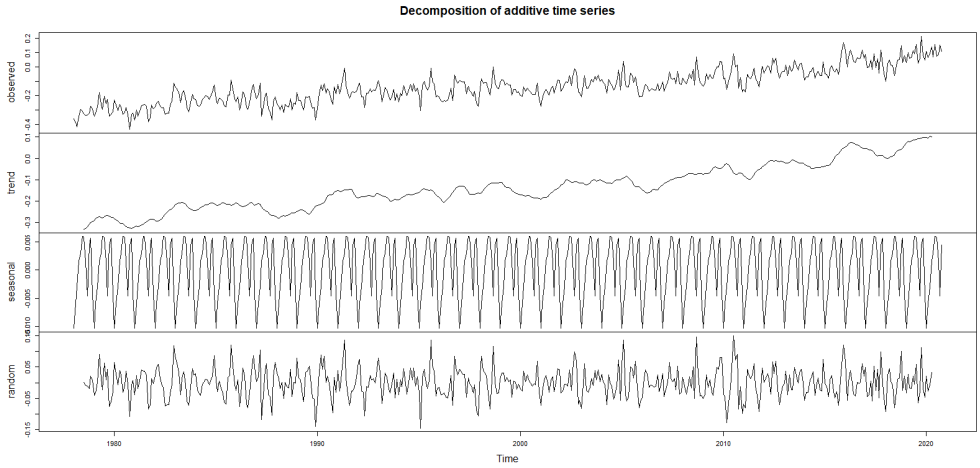

Figure 4. Decomposition of Monthly Mean Sea Level at Grand Isle, Louisiana, January 1978 ~ October 2020 (Source: own calculations)

One of the main objectives for a decomposition is to estimate seasonal effects that can be used to create and present seasonally adjusted values. Seasonal adjustment is the estimation and removal of seasonal effects that are not explainable by the dynamics of trends or cycles from a time series to reveal certain non-seasonal features. This can be done by subtracting the estimated seasonal component from the original time series. After removed the seasonal variation, the seasonally adjusted time series only contained the trend component and an irregular component (Figure 5).

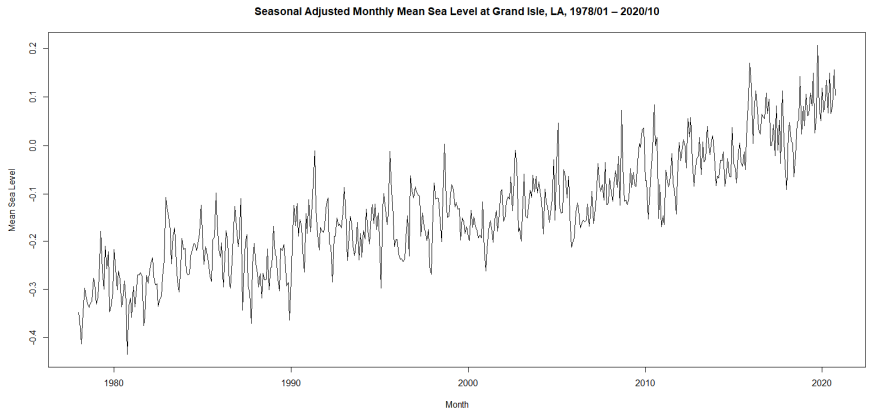

Figure 5. Time Series Plot of Seasonal Adjusted Monthly Mean Sea Level at Grand Isle, Louisiana, January 1978 ~ October 2020 (Source: own calculations)

By looking at the time series plot of the data, the ACF is useful for identifying non-stationary time series. For a stationary time series, the ACF will drop to zero relatively quickly, while the ACF of non-stationary data decreases slowly. The ACF (Figure 6) of the time series, seasonal adjusted monthly mean sea level from January 1978 to October 2020 at Grand Isle, Louisiana, showed strong positive statistically significant correlations at up to 24 lags that never decay to zero. This also illustrated by the single spike at the first lag followed by small apparently random values after the first lag for the PACF (Figure 7). Typically, the ACF and PACF shown in Figures 6 and 7 were a time series that has autocorrelation at the first lag only. Since the PACF cut off after the first lag, it seems that the time series followed AR(1) model.

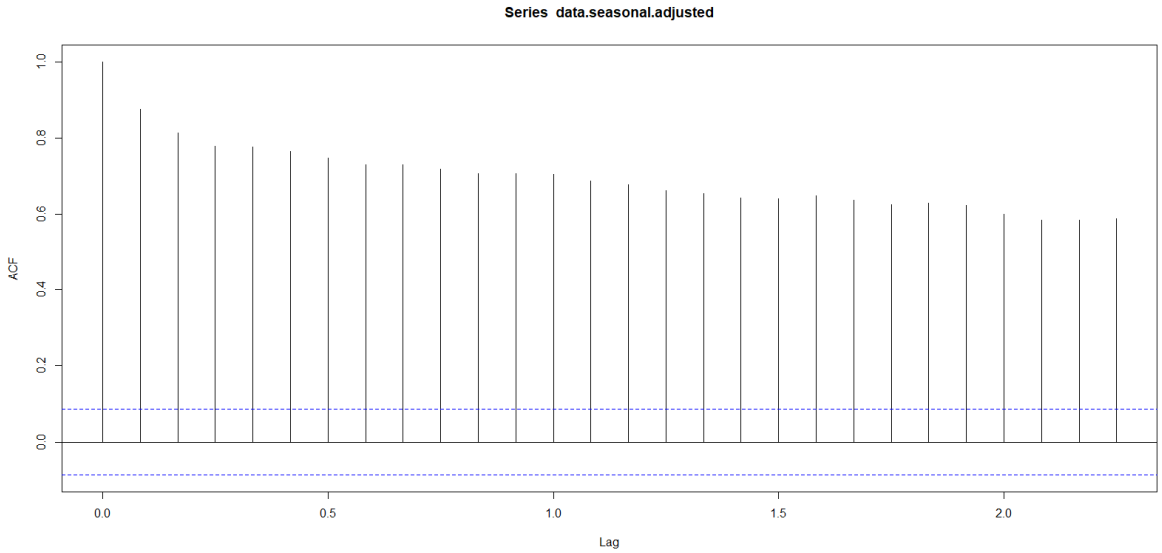

Figure 6. ACF Plot of Seasonal Adjusted Monthly Mean Sea Level at Grand Isle, Louisiana, January 1978 ~ October 2020 (Source: own calculations)

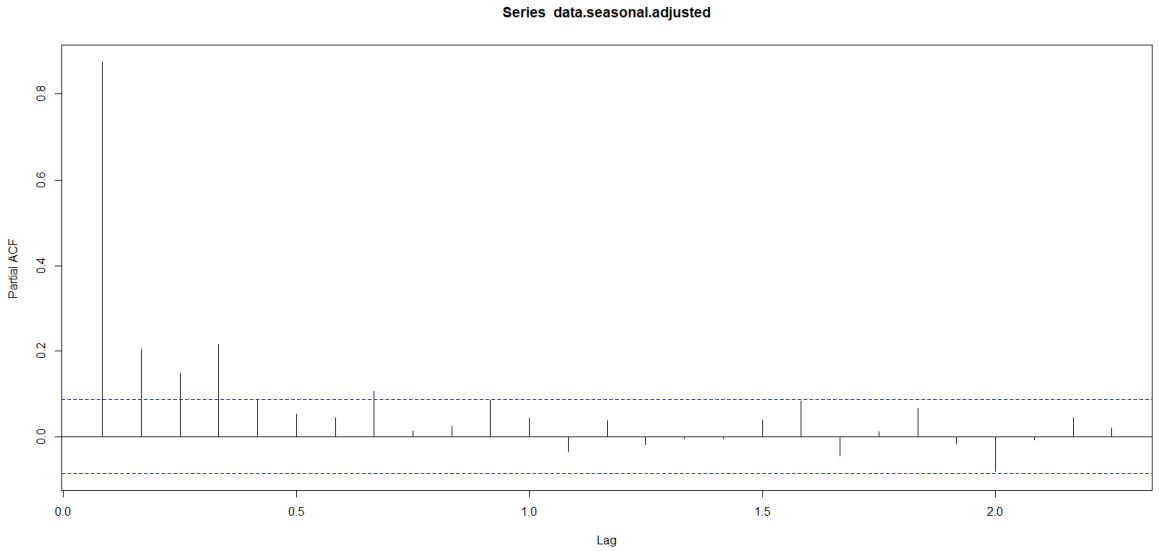

Figure 7. PACF Plot of Seasonal Adjusted Monthly Mean Sea Level at Grand Isle, Louisiana, January 1978 ~ October 2020 (Source: own calculations)

In terms of non-stationary time series, differencing can be used to transform a non-stationary time series into a stationary one. When both trend and seasonality are present, we may need to apply both a non-seasonal first difference and a seasonal difference. The first difference of a time series is the time series of changes from one period to the next. Notice that the graph of the first difference of the time

series, seasonal adjusted monthly mean sea level from January 1978 to October 2020 at Grand Isle, Louisiana, looked approximately stationary (Figure 8). According to the Augmented Dickey-Fuller Test, Dickey-Fuller = -11.944 with lag order = 7 and the p-value of the test was smaller than **0.01. It rejected the null hypothesis that is non-stationary, and** suggested that the first difference of the time series was stationary.

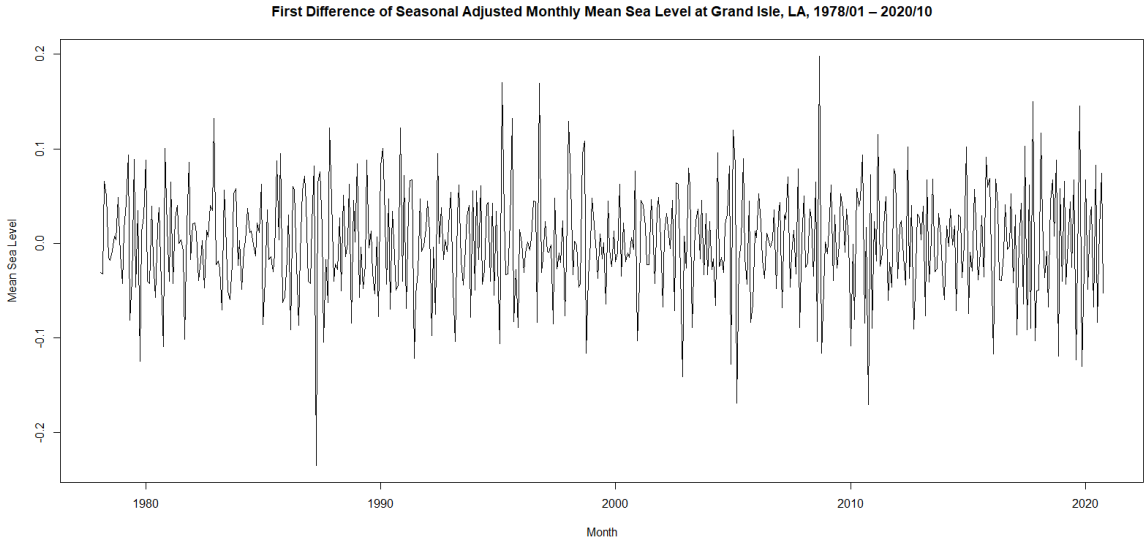

Figure 8. Time Series Plot of First Difference of Seasonal Adjusted Monthly Mean Sea Level at Grand Isle, Louisiana, January 1978 ~ October 2020 (Source: own calculations)

Stationarizing a time series through differencing is an important part of the process of fitting an ARIMA model. The ACF of first difference shown in Figure 9 showed a significant positive spike at the first lag followed by correlations that were statistically significant. The corresponding PACF of first difference in Figure 10 showed most likely a gradual decrease after the first few lags. Since the ACF cut off after the first lag and the PACF decrease gradually, a reasonable conclusion was that the first differenced time series followed MA(1) model.

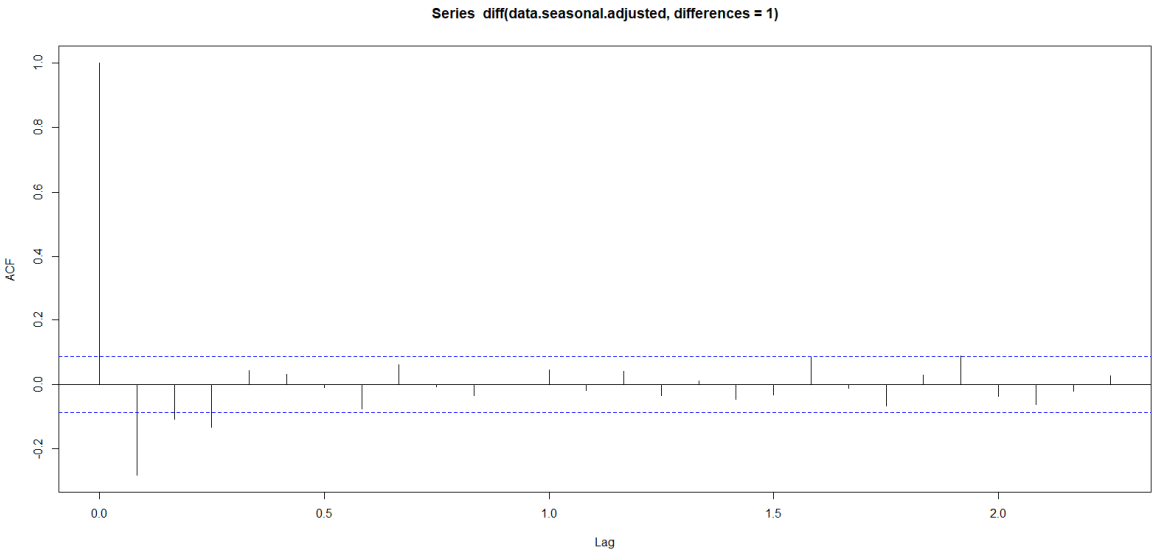

Figure 9. ACF Plot of First Difference of Seasonal Adjusted Monthly Mean Sea Level at Grand Isle, Louisiana, January 1978 ~ October 2020 (Source: own calculations)

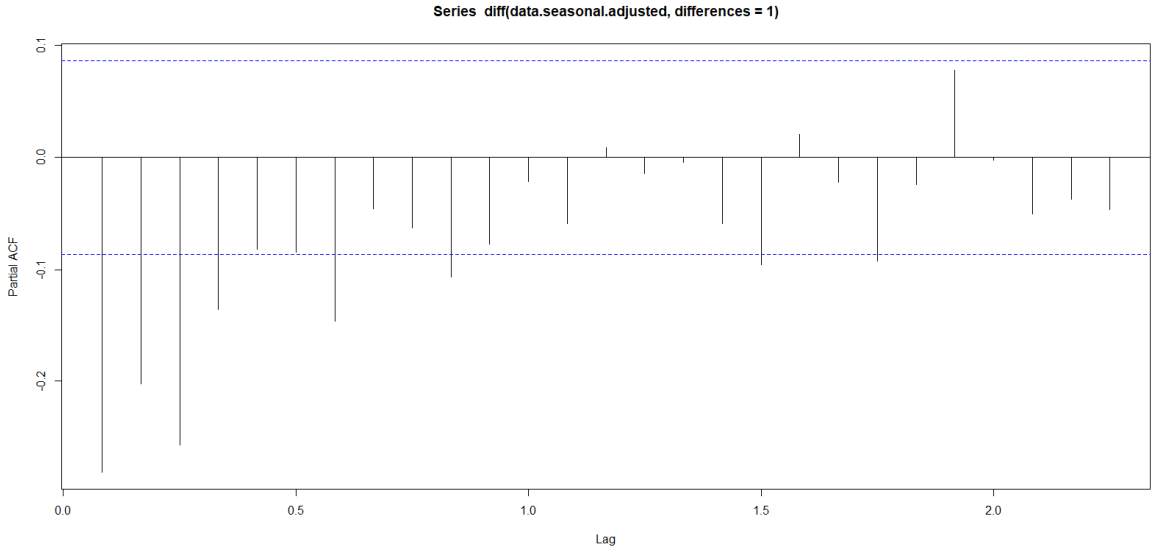

Figure 10. PACF Plot of First Difference of Seasonal Adjusted Monthly Mean Sea Level at Grand Isle, Louisiana, January 1978 ~ October 2020 (Source: own calculations)

Seasonal differencing can remove seasonal trend and can also get rid of a seasonal random walk type of non-stationarity. Seasonal differencing is defined as a difference between a value and a value with lag that is a multiple of seasonality (S). In this case, S = 12 (months per year) is the span of the periodic seasonal behavior. Figure 11 showed the graph of the 12th difference of the time series, which looked approximately stationary. Meanwhile, the test statistic of the Augmented Dickey-Fuller Test was Dickey-Fuller = -37.923 with lag order = 7 and the p-value of the test was smaller than **0.01. It rejected the null hypothesis that is non-stationary, and** suggested that the 12th first difference of the time series was stationary.

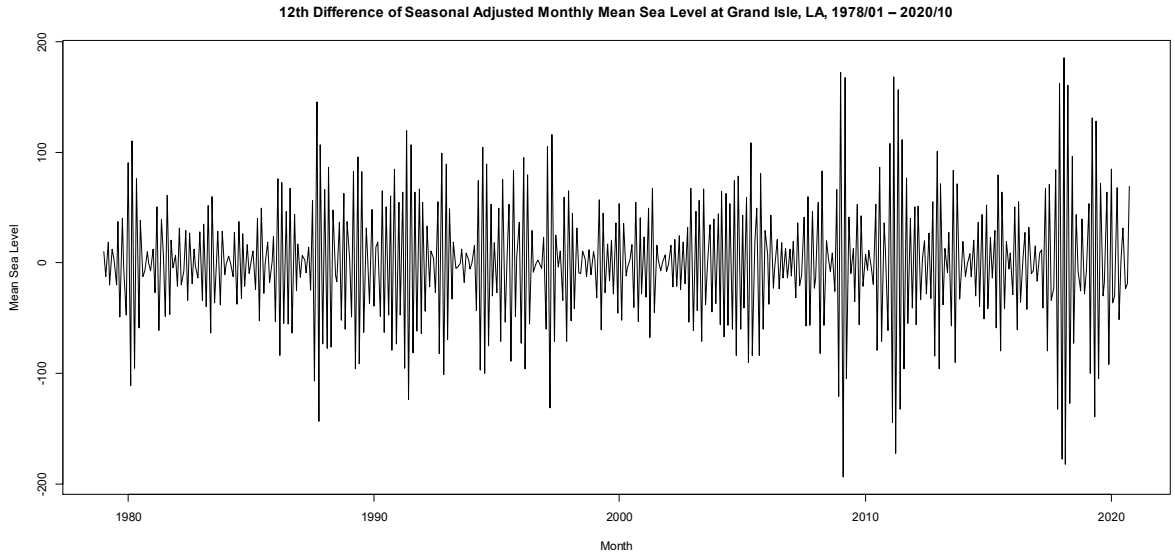

Figure 11. Time Series Plot of 12th Difference of Seasonal Adjusted Monthly Mean Sea Level at Grand Isle, Louisiana, January 1978 ~ October 2020 (Source: own calculations)

Figure 12 showed what ACF most likely a steady decay after the first few lags and bounce around between being positive and negative statistically significant. Meanwhile, Figure 13 showed what PACF mostly looks like a steady negative decay in the partial correlations toward zero. This is consistent with the general recommendation that if the autocorrelation at the first seasonal lag is positive we should use an autoregressive (AR) model vs. a moving average (MA) model.

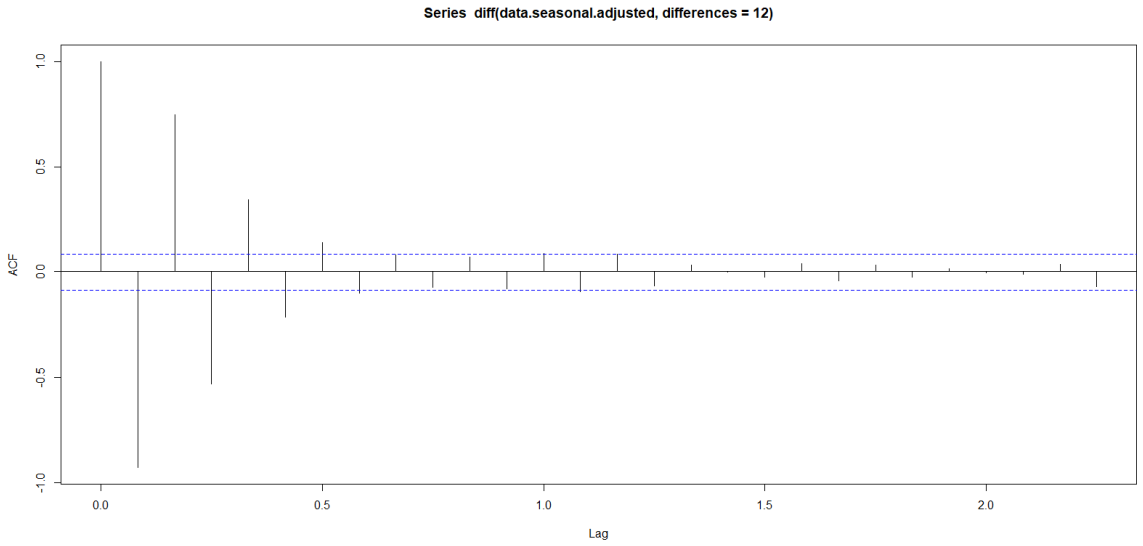

Figure 12. ACF Plot of 12th Difference of Seasonal Adjusted Monthly Mean Sea Level at Grand Isle, Louisiana, January 1978 ~ October 2020 (Source: own calculations)

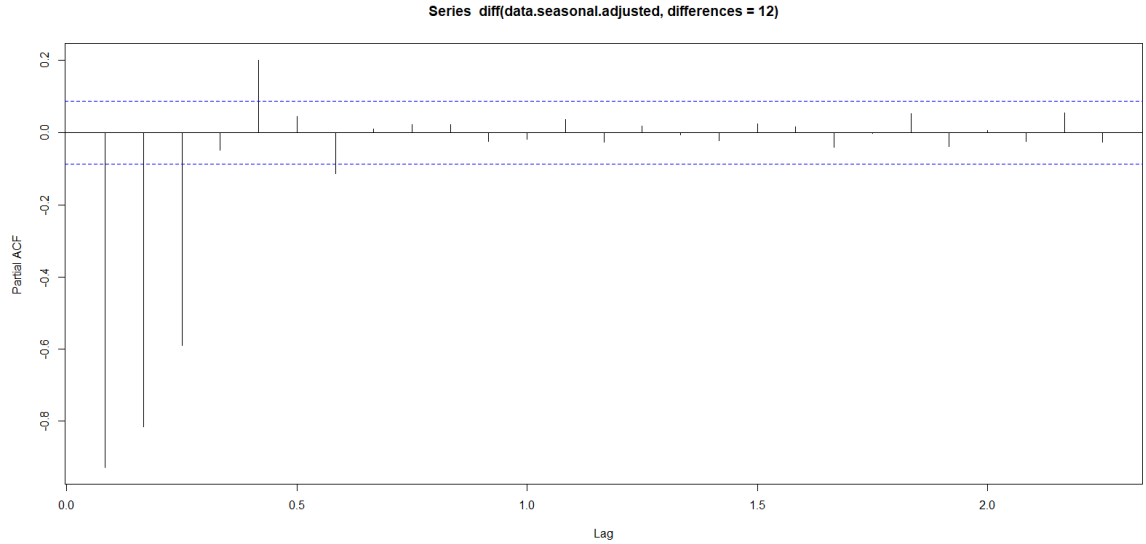

Figure 13. PACF Plot of 12th Difference of Seasonal Adjusted Monthly Mean Sea Level at Grand Isle, Louisiana, January 1978 ~ October 2020 (Source: own calculations)

4.2 Estimation of the Seasonal ARIMA Model Parameters

Empirically, the choice of the model order is somewhat arbitrary. While for the decision for the seasonal ARIMA model, this is where practical aspects, which means that the fitting seasonal ARIMA model should come to play as well. One of the main challenges of forecasting with the seasonal ARIMA model is the cumbersome tuning process of the models. In order to find a solution, the auto.arima() function from the "forecast" package in R 4.0.2 for Windows was employed to identify both the structure of the series (stationary or not) and type (seasonal or not), and sets the model's parameters, that takes into account the AIC, AICc or BIC values generated to determine the best fitting seasonal ARIMA model.

Consequently, the ARIMA (1,1,1)(2,0,0)[12] with drift model was selected to be the best fitting model for the time series, according to the lowest AIC value (-1612.92) in this study. Given this option, the ARIMA (1,1,1)(2,0,0)[12] with drift model was chosen for further forecasting process, and the parameters of the ARIMA(1,1,1)(2,0,0)[12] with drift model were presented in Table 1. The ARIMA (1,1,1)(2,0,0)[12] with drift model would yield the following forecasting equation:

$$(1 - \phi_1 B)(1 - B)(1 - \Phi_1 B^{12} - \Phi_2 B^{24})\hat{Y}_t = c + (1 - \theta_1 B)$$

The ARIMA(1,1,1)(2,0,0)[12] with drift model for the time series, seasonal adjusted monthly mean sea level from January 1978 to October 2020 at Grand Isle, Louisiana, can be expressed as follows:

$$(1 - 0.4627B)(1 - B)(1 - 0.0542B^{12} + 0.0647B^{24})\hat{Y}_t = 0.0008 + (1 + 0.9671B)$$

Table 1. Parameters of the ARIMA(1,1,1)(2,0,0)[12] with Drift Model

Parameter	Estimate	Standard Error
Constant	8e-04	2e-04
AR Lag 1	0.4627	0.0449
Difference	1	
MA Lag 1	-0.9671	0.0160
SAR1	0.0542	0.0451
SAR2	-0.0647	0.0457
$Sigma^2$ estimated as 0.00248, Log Likelihood = 812.46		
AIC = -1612.92, AICc = -1612.76, BIC = -1587.48		
RMSE = 0.04951302, MSE = 0.00245154, MAE = 0.03865538, MAPE = 96.94481		

Source: own calculations

4.3 Diagnostic Checking of the Seasonal ARIMA Model

A common task when building forecasting model is to check that the residuals satisfy some assumptions that they are uncorrelated, normally distributed, etc. The top figure of Figure 14 showed that the residuals from the ARIMA(1,1,1)(2,0,0)[12] with drift model did not violate the assumption of constant location and scale. The bottom right figure of Figure 14 showed that the residual histogram did not reveal a series deviation from normality in this case. The ACF plot of the residuals (the bottom left figure of Figure 14) from the ARIMA(1,1,1)(2,0,0)[12] with drift model showed that all sample autocorrelations were within the threshold limits, indicating that the residuals appeared to be random.

The Ljung–Box Q–test (Ljung & Box, 1978) is a diagnostic tool used to test the lack of fit of a time series model. In this example, the test statistic of the Ljung–Box Q–test was Q = **20.637** with 19 degrees of freedom and the p-value of the test was **0.3572 (model degrees of freedom: 5, total lags used: 24), indicating that the residuals were random and that the model provided an adequate fit to the data.** This, combined with the Ljung–Box Q–test statistic, suggested that the ARIMA(1,1,1)(2,0,0)[12] with drift model appropriately modeled the dynamics for this time series.

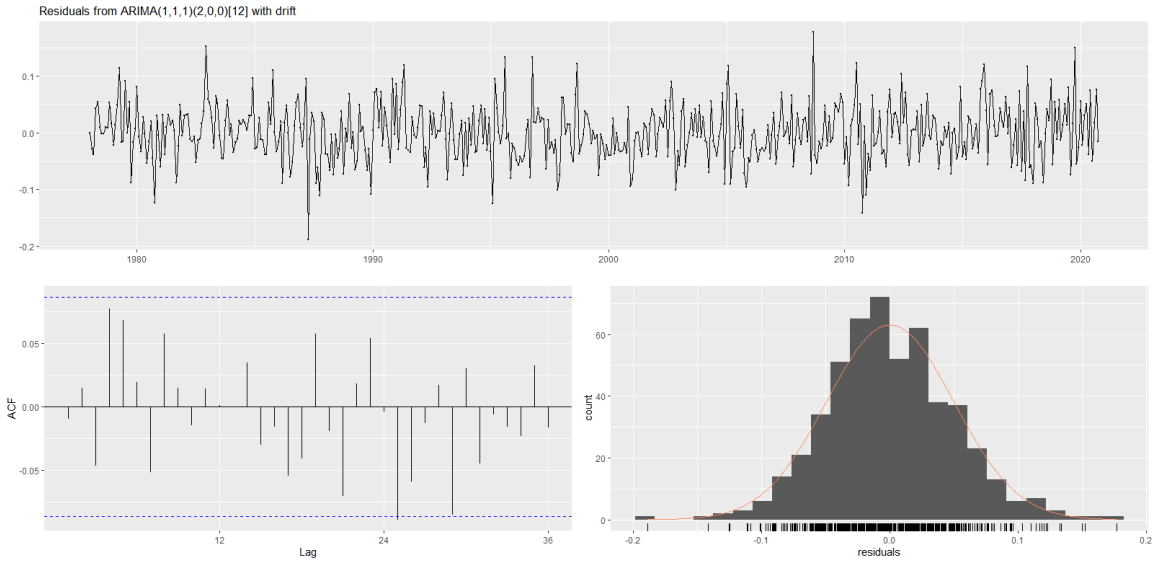

Figure 14. Residuals of ACF and PACF (Source: own calculations)

4.4 Using the Seasonal ARIMA Model in Forecasting Process

The forecasted values of monthly mean sea level at Grand Isle, Louisiana were shown in Table 2. Forecasts from the chosen model, the ARIMA(1,1,1)(2,0,0)[12] with drift model, were shown in Figure 15. It showed a linear upward trend projected into the future. The following figure (Figure 16) illustrated that the black line represented the visuals of monthly mean sea level dataset without forecasting and the red line represented the visuals of monthly mean sea level dataset with forecasted values. Forecasting process with the ARIMA(1,1,1)(2,0,0)[12] with drift model indicated a good fitting of the model for forecasting at a constant increasing rate in the short-term.

Table 2. Forecasted Values of Monthly Mean Sea Level at Grand Isle, Louisiana (mm/year)

Date	Point Forecast	95% Lower Control Limit	95% Upper Control Limit
November 2020	0.09365086	-0.00396428	0.1912660
December 2020	0.08403179	-0.02491547	0.1929790
January 2021	0.08867724	-0.02323735	0.2005918
February 2021	0.08141552	-0.03150764	0.1943387
March 2021	0.08599300	-0.02738818	0.1993742
April 2021	0.08852848	-0.02512923	0.2021862
May 2021	0.08266219	-0.03120353	0.1965279
June 2021	0.08957847	-0.02446676	0.2036237
July 2021	0.08144601	-0.03276613	0.1956582
August 2021	0.09111014	-0.02326314	0.2054834
September 2021	0.09350632	-0.02102534	0.2080380
October 2021	0.08203079	-0.03265786	0.1967195
November 2021	0.09070678	-0.02453532	0.2059489
December 2021	0.09265510	-0.02290795	0.2082181
January 2022	0.08935230	-0.02644549	0.2051501
February 2022	0.09293820	-0.02305891	0.2089353
March 2022	0.09222405	-0.02395685	0.2084049
April 2022	0.09065890	-0.02569866	0.2070165
May 2022	0.09549201	-0.02103886	0.2120229
June 2022	0.09128139	-0.02542109	0.2079839
July 2022	0.09704305	-0.01983014	0.2139162
August 2022	0.09729601	-0.01974734	0.2143394
September 2022	0.09341817	-0.02379496	0.2106313
October 2022	0.09701416	-0.02036842	0.2143967

Source: own calculations

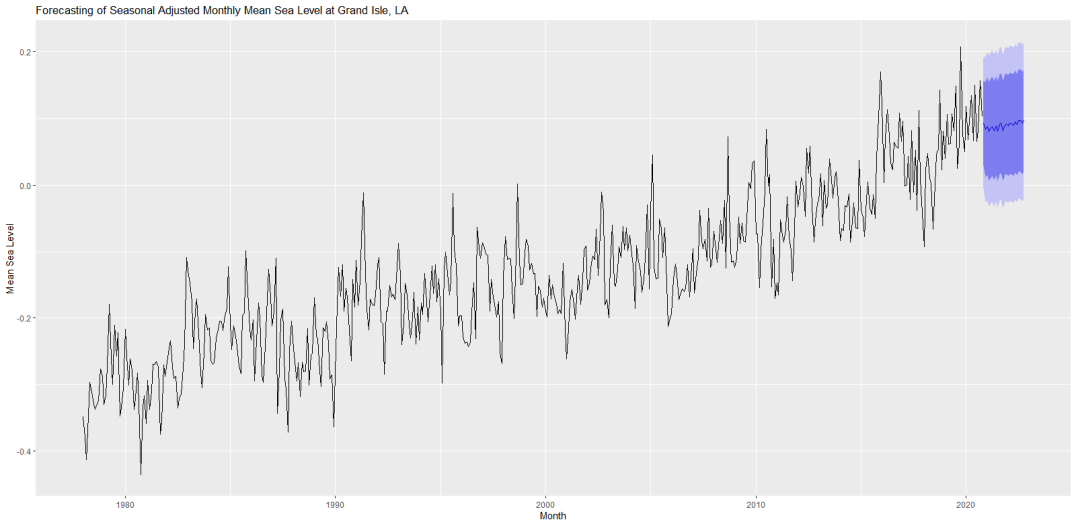

Figure 15. Observed and Forecasted Monthly Mean Sea Level at Grand Isle, Louisiana (Source: own calculations)

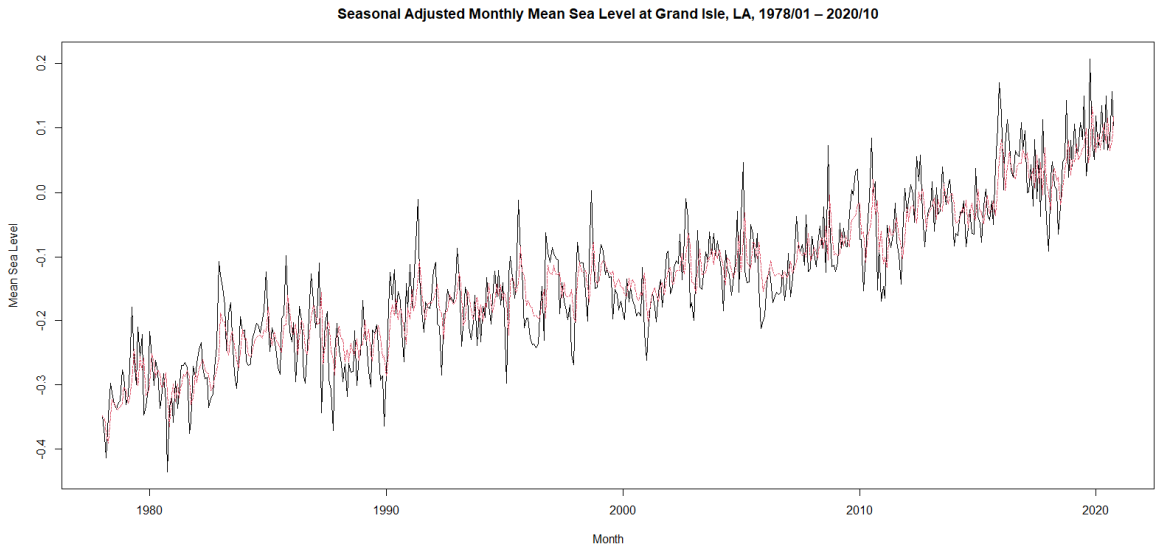

Figure 16. Observed and Forecasted Monthly Mean Sea Level at Grand Isle, Louisiana
(Source: own calculations)

4.5 Multilayer Perceptron Neural Network Model

Neural network is one of the most popular machine learning methods, which is able to do prediction tasks in a more reliable manner. Gardner and Dorling (1998) define multilayer perceptron (MLP) as: "a system of simple interconnected neurons, or nodes, which is a model representing a nonlinear mapping between an input vector and an output vector". MLP consists of three layers of nodes: an input layer, a hidden layer and an output layer (Figure 17). Except for the input nodes, each node is a neuron that uses a nonlinear activation function.

MLP utilizes a supervised learning technique called backward propagation to analyze the dataset in three stages. The first stage is the "training process" that tries to perceive the association between the variables in the dataset. Based on this learning outcome, it will attempt to discern a model and it is done in a hidden layer called hidden/perceptron process. In this process, the optimal functions in the model are produced and dependent variables are assigned weights. In the third stage, new model is estimated called as the output process (Manel et al., 1999).

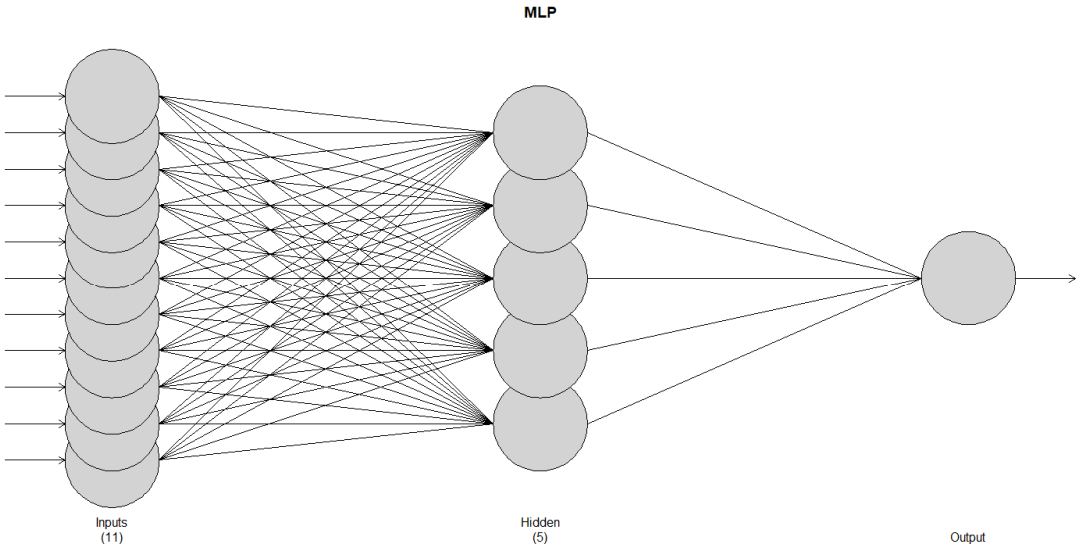

Figure 17. Single Hidden Layer MLP
(Source: own calculations)

MLP is trained for multi-step ahead prediction. On testing as well as training data sets for short-term prediction. Thus, the optimum neural network model is proposed for short-term prediction of the time series. In this case, training was performed using the time series, seasonal adjusted monthly mean sea level from January 1978 ~ December 2010, and testing was performed using the time series, seasonal adjusted monthly mean sea level from January 2011 ~ December 2020.

The mlp() function from the "nnfor" package in R 4.0.2 for Windows automatically generates ensembles of networks, the training of which starts with different random initial weights. Training process categorized into two main steps: first is to select the best architecture of networks, and second is to integrate MLP with optimizers. The output indicated that the resulting MLP model has 5 hidden nodes, it was trained 20 times and the different forecasts were combined using the median operator (Figure 17). The results were compared with reference to the MSE (mean square error) = 0.0015 against the ARIMA(1,1,1)(2,0,0)[12] with drift model, MSE = 0.00245154.

The top figure of Figure 18 showed that the residuals from the MLP model did not violate the assumption of constant location and scale. The bottom right figure of Figure 18 showed that the residual histogram from the MLP model did not reveal a series deviation from normality. At the same time, the ACF plot of the residuals (the bottom left figure of Figure 18) from the MLP model showed that all sample autocorrelations were within the threshold limits, indicating that the residuals appeared to be random.

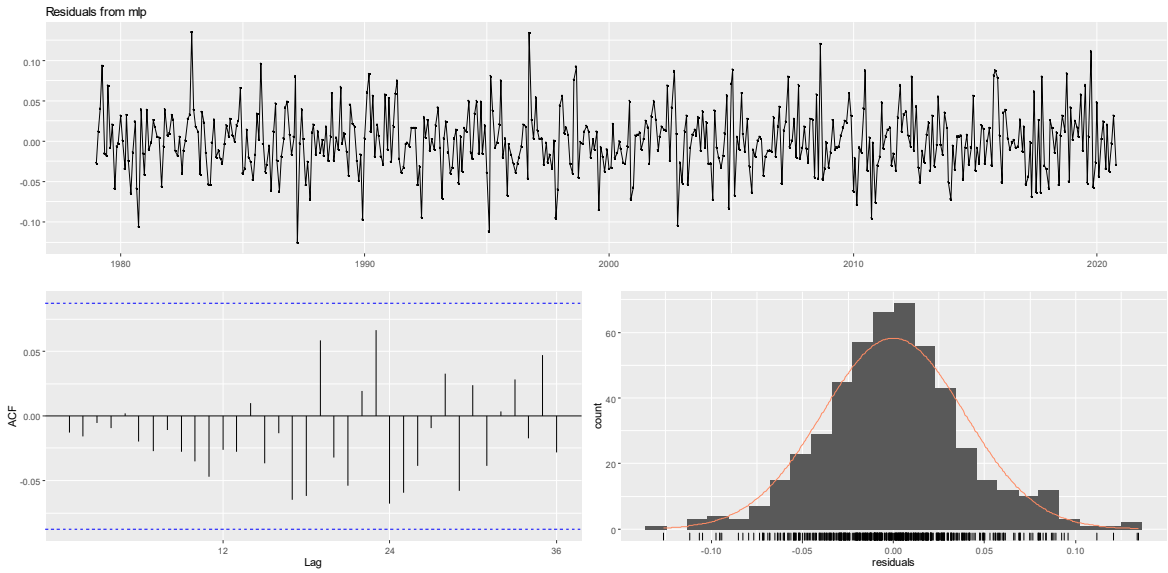

Figure 18. Residuals of ACF and PACF
(Source: own calculations)

The MLP forecasted values of monthly mean sea level at Grand Isle, Louisiana were shown in Table 3. Forecasts from the MLP model were also shown in Figure 19. It showed a linear upward trend projected into the future. Forecasting process with the MLP model indicated a good fitting of the model for forecasting at a constant increasing rate in the short-term.

Table 3. Multilayer Perceptron Neural Network Forecasted Values of Monthly Mean Sea Level at Grand Isle, Louisiana (mm/year)

	2020	2021	2022	2023	2024	2025
January	---	0.09936061	0.12674511	0.14594009	0.16597423	0.19751233
February	---	0.11719078	0.12637860	0.15971546	0.18860363	0.19918627
March	---	0.12194357	0.13726855	0.15939375	0.17982793	0.21593495
April	---	0.10240746	0.13142455	0.15684624	0.17054913	0.21139992

May	---	0.12296535	0.12539289	0.15846142	0.18101449	0.21478198
June	---	0.11358740	0.12939848	0.14588277	0.18099360	0.22616180
July	---	0.11091493	0.13369095	0.17559040	0.19196263	0.22387009
August	---	0.11783468	0.14661229	0.17653542	0.20409253	0.22334760
September	---	0.13477446	0.13901352	0.18113330	0.21136700	0.23402481
October	---	0.12605342	0.13694346	0.16952613	0.20328672	0.23474498
November	0.09208658	0.13968442	0.14800607	0.17043035	0.19742043	---
December	0.10225777	0.12685689	0.14909446	0.17386078	0.19478678	---

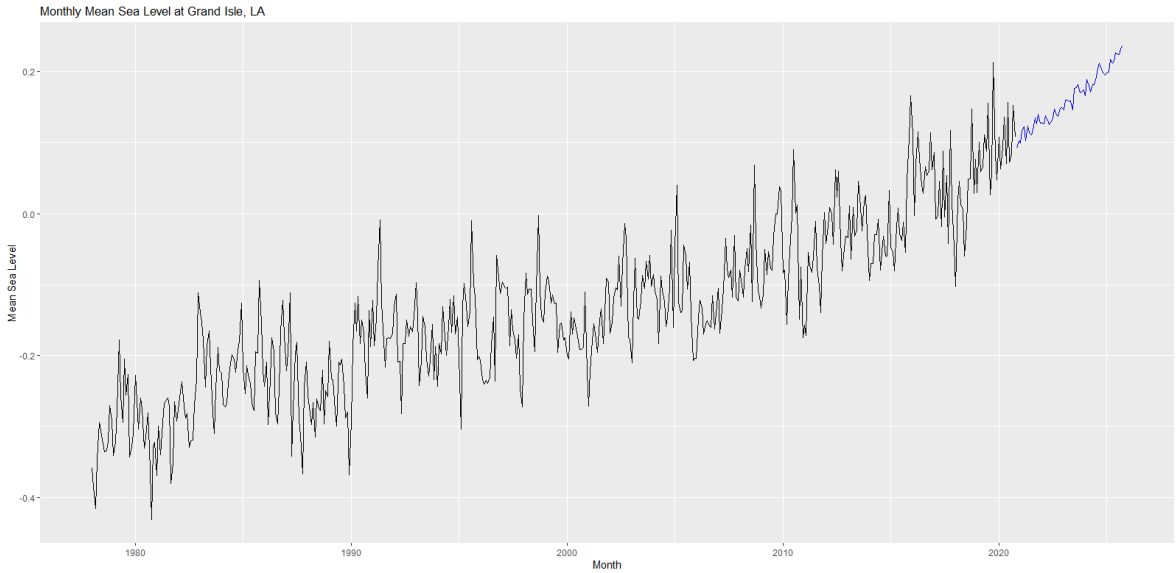

Figure 19. Observed and Forecasted Monthly Mean Sea Level at Grand Isle, Louisiana (Source: own calculations)

5. Discussion

There were many studies concluded that global sea level is rising at an increasing rate. While sea level changes are a relatively slow process, therefore, understanding past sea level is important for the analysis of current and future sea level changes. In order to sustain these observations, research programs utilizing the existing data should be able to improve our understandings and narrow projections of future sea level changes significantly.

Sea level changes are driven by a variety of mechanisms operating at different spatial and temporal scales (Kopp et al., 2015). Furthermore, forecasting future relative sea level changes at specific locations requires not just an estimate of global mean sea level changes, but also estimates of the different processes contributing to global mean sea level changes, as well as of the processes contributing exclusively to regional or local mean sea level changes (Kopp et al., 2015).

Tides, for example, are predictable because of the occurrence by a combination of forces, particularly the earth and the moon in relation to the sun. Local mean sea level can be measured at tide stations, which refers to the height of the water as measured along the coast relative to a specific point on land. To understand tides, it is important to understand the movements of the earth and the moon relative to the sun. However, most of the time, and in most places, tides are much more complex.

6. Conclusion

In this study the best choice time series model was the ARIMA (1,1,1)(2,0,0)[12] with drift model as its lowest AIC values among other models. It was noticed that this ARIMA (1,1,1)(2,0,0)[12] with drift model gave evidence about future monthly mean sea level would increase over time at Grand

Isle, Louisiana. Prediction is a kind of dynamic filtering, in which past values of one or more time series are used to predict future values. Currently, neural network is one of the most popular machine learning methods, which is able to do prediction tasks in a more reliable manner. With time series data, lagged values of the time series can be used as inputs to a neural network, the MLP neural network was applied to time series prediction using its past values of a univariate time series in this study. Empirically, the results revealed that the MLP neural network model performed better compared to the ARIMA(1,1,1)(2,0,0)[12] with drift model at its smaller MSE value. Hence, the MLP neural network model not only can provided information which are important in decision making process related to the future sea level change impacts, but also can be employed in forecasting the future performance for local mean sea level change outcomes. For the further research tasks, the nonlinear autoregressive (NAR) neural network with different algorithm methods can be used to understand current and past information of the same time series (monthly mean sea level) in terms of forecasting accuracy consideration.

JEL Classification

C22, C45, C53, Q54

References

[1] Bolin, D., Guttorp, P., Januzzi1, A., Jones1, D., Novak1, M., Podschwit, H., Richardson, L., S¨arkk¨a, A., Sowder, C., & Zimmerman, A. (2015). Statistical prediction of global sea level from global temperature. *Statistica Sinica*, 25, 351-367.

[2] Box, G.E.P., & Jenkins, G.M. 1970. *Time series analysis: forecasting and control*. Holden-Day, San Francisco.

[3] Box, G.E.P., Jenkins, G.M., Reinsel,G.C., & Ljung, G.M. (2016). *Time series analysis: forecasting and control* (5th ed.). Hoboken, N.J.: John Wiley and Sons Inc.

[4] Braakmann-Folgmann, A., Roscher, R., Wenzel, S., Uebbing, B., & Kusche, J. (2017). *Sea level anomaly prediction using recurrent neural networks*. In Proceedings of the 2017 Conference on Big Data from Space, pp. 297-300.

[5] Bruneau, N., Polton,J., Williams, J., & Holt, J. (2020). Estimation of global coastal sea level extremes using neural Networks. *Environmental Research Letters*, 15(7), 074030, 1-11.

[6] Cazenave, A., & Llovel, W. (2010). Contemporary sea level rise. *Annual Review of Marine Science*, 2, 145-173.

[7] Cazenave, A., & Cozannet, G.L. (2013). Sea level rise and its coastal impacts. *Earth's Future*, 2, 15–34.

[8] Church, J.A., White, N.J., Coleman, R., Lambeck, K., & Mitrovica, J.X. (2004). Estimates of the regional distribution of sea level rise over the 1950-2000 period. *Journal of Climate*, 17(13), 2609-2625.

[9] Church, J.A., & White, N.J. (2006). A 20th century acceleration in global sea-level rise. *Geophysical Research Letters*, 33, L01602, 1-4.

[10] Church, J.A., White, N.J., Aarup, T., Wilson, W.S., Woodworth, P.L., Domingues, C.M., Hunter, J.R., & Lambeck, K. (2008). Understanding global sea levels: past, present and future. *Sustainability Science*, 3, 9-22.

[11] Church, J.A., & White, N.J. (2011). Sea-level rise from the late 19th to the early 21st century. *Surveys in Geophysics*, 32, 585-602.

[12] Foster, G., & Brown, P.T. (2014). Time and tide: analysis of sea level time series. *Climate Dynamics*, 45, 1-2, 291-308.

[13] Gardner, M.W., & Dorling, S.R. (1998). Artificial neural networks (the multilayer perceptron) - a review of applications in the atmospheric sciences. *Atmospheric Environment*, 32(14), 2627-2636.

[14] Haasnoot, M., Kwadijk, J., Alphen, J., Bars, D., Hurk, B., Diermanse, F.,Spek, A., Essink, G.O., Delsman, J., & Mens, M. (2020). Adaptation to uncertain sea-level rise; how uncertainty in Antarctic mass-loss impacts the coastal adaptation strategy of the Netherlands. *Environmental Research Letters*, 15, 034007, 1-15.

[15] Horton, B.P., Kopp, R.E., Garner, A.J., Hay, C.C. Khan, N.S., Roy, K., & Shaw, T.A. (2018). Mapping sea-level change in time, space, and probability. *Annual Review of Environment and Resources*, 43, 481-521.

[16] IPCC. (2014). *Climate Change 2014: Synthesis Report*. Contribution of Working Groups I, II and III to the Fifth Assessment Report of the Intergovernmental Panel on Climate Change [Core Writing Team, PachauriR.K., & Meyer, L.A. (eds.)], IPCC, Geneva, Switzerland, 151 pp.

[17] Kopp, R.E., Horton,B.P., Kemp, A.C., & Tebaldi, C. (2015). Past and future sea level rise along the coast of North Carolina, USA. *Climatic Change*, 132, 693–707.

[18] Kopp, R.E., Hay, C.C., Little, C.M., & Mitrovica, J.X. (2015). Geographic variability of sea-level change. *Current Climate Change Reports*, 1, 192–204.

[19] Kulp, S.A., & Strauss, B.H. (2019). New elevation data triple estimates of global vulnerability to sea-level rise and coastal flooding. *Nature Communications*, 10, 4844, 1-12.

[20] Ljung, G.M., & Box, G.E.O. (1978). On a measure of lack of fit in time series models. *Biometrika*, 65(2), 297-303.

[21] Makarynskyy, O., Makarynska, D., Kuhn, M., & Featherstone, W.E. (2004). Predicting sea level variations with artificial neural networks at Hillarys Boat Harbour, Western Australia. Estuarine. *Coastal and Shelf Science*, 61(2), 351–360.

[22] Manel, S., Dias, J.M., Buckton, S.T., & Ormerod, S.J. (1999). Alternative methods for predicting species distribution: an illustration with Himalayan river birds. *Journal of Applied Ecology*, 36, 734–747.

[23] Montgomery, D.C., Jennings, C.L., & Kulahci, M. (2008). *Introduction to time series analysis and forecasting*. Hoboken, N.J.: John Wiley & Sons. Inc.

[24] Neumann, J.E., Yohe, G., Nicholls, R., & Manion, M. (2020). *Sea level rise & global climate change: A review of impacts to U.S. coasts*. The Center for Climate and Energy Solutions prepared for the Pew Center on Global Climate Change, 38 pp.

[25] Srivastava, P.K., Islam, T., Singh, S.K., Petropoulos, G.P., Gupta, M., & Dai, Q. (2016). Forecasting Arabian sea level rise using exponential smoothing state space models and ARIMA from TOPEX and Jason satellite radar altimeter data. *Meteorological Applications*, 23, 633-639.

[26] U.S. Global Change Research Program (USGCRP). (2017). *Climate science special report: Fourth National Climate Assessment, Volume I*. [Wuebbles, D.J., Fahey, D.W., Hibbard, K.A., Dokken, D.J., Stewart, B.C., & Maycock, T.K. (eds.)], U.S. Global Change Research Program, Washington, DC, USA, 470 pp.

[27] Visser, H., Dangendorf, S., & Petersen, A.C. (2015). A review of trend models applied to sea level data with reference to the "acceleration-deceleration debate". *Journal of Geophysical Research: Oceans*, 120(6), 3873-3895.

[28] Wang, W., & Yuan, H. (2018). A tidal level prediction approach based on BP neural network and Cubic B-Spline Curve with Knot Insertion Algorithm. *Mathematical Problems in Engineering*, 2018, Article ID 9835079, 9 pp.